

# Coagulation Rate Studies of Spinnable Chitosan Solutions

JONATHAN Z. KNAUL, KATHERINE A. M. CREBER

Department of Chemistry and Chemical Engineering, Royal Military College of Canada, P.O. Box 17000, Stn. Forces, Kingston, Ontario, K7K 7B4 Canada

Received 31 October 1996; accepted 3 March 1997

**ABSTRACT:** The coagulation properties of some mixtures of 5% chitosan in 2% aqueous acetic acid were investigated with the goal of determining the optimal coagulation conditions for the spinning of chitosan fibers. The chitosan was characterized and found to possess a deacetylation value of  $84.9 \pm 0.2\%$ . Molecular weight of the chitosan was also measured; based on intrinsic viscosity, the  $M_v$  value was  $7.73 \times 10^5 \text{ g mol}^{-1}$ , and based on high-pressure liquid chromatography, the  $M_w$  value was  $1.14 \times 10^5 \text{ g mol}^{-1}$ . Solutions of 5% chitosan/2% acetic acid were prepared, filtered, and extruded through a large-diameter hole syringe into coagulation baths of varying composition that were all strongly basic in nature, at least a pH of 12 or greater. For each coagulant, time was varied from between 22 s and 2 minutes at room temperature. A second set of experiments was conducted where the temperature was varied from 20°C to 70°C at a constant time of 45 s. In a third set of experiments, using a 1M NaOH coagulant, different chitosans were also analyzed. Throughout all of the experiments, a distinct moving boundary between coagulated and uncoagulated polymer was observed within the cylindrical-shaped polymer fibers. Using a series of equations based on Fick's 2nd Law, a straight line relationship has been demonstrated between boundary motion and time and between boundary motion and temperature for each coagulant tested. The activation energy for each coagulant was also determined. © 1997 John Wiley & Sons, Inc. *J Appl Polym Sci* **66**: 117–127, 1997

**Key words:** chitosan; coagulation; diffusion; deacetylation; boundary

## INTRODUCTION

Chitin, a (1-4)-linked 2-acetamido-2-deoxy- $\beta$ -D-glucan, is a natural polysaccharide that occurs mainly in insects, marine invertebrates, fungi, and yeasts. It is the second most abundant natural polymer, cellulose being the most abundant.<sup>1</sup> Chitosan is the *N*-deacetylated derivative of chitin, although 100% *N*-deacetylation is almost never achieved. It is generally accepted that this biopolymer is referred to as "chitosan" if chitin is *N*-deacetylated to such a degree that it becomes soluble in dilute aqueous acidic systems. Structural examples of chi-

tin, chitosan, and the structurally similar biopolymer cellulose can be found in Figure 1. While chitosan holds great potential as a production fiber, it is still a research product. In order to extrude chitosan fibers, the extrudate may undergo either a wet spinning or dry-jet wet spinning process. In both cases, the chitosan is typically dissolved in an acidic solution and then extruded into a basic coagulation bath where the chitosan is expected to precipitate out of solution, in the form of a fiber. The precipitated fiber may be subsequently washed, dried, and taken up on a winder.

In the coagulation bath, two processes for removal of the solvent and solidification of the dissolved polymer are possible: either by a chemical reaction between solvent and coagulant or by a physical exchange of solvent and nonsolvent, resulting in precipitation of the polymer. An exam-

Correspondence to: J. Z. Knaul.

*Journal of Applied Polymer Science*, Vol. 66, 117–127 (1997)  
© 1997 John Wiley & Sons, Inc. CCC 0021-8995/97/010117-11

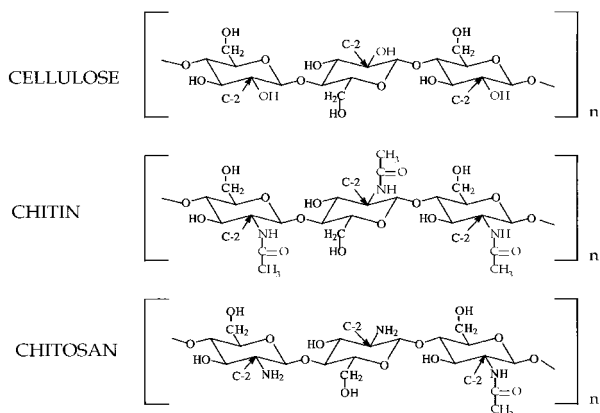
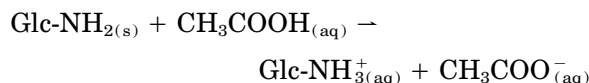


**Figure 1** Segments of chitin, chitosan, and cellulose polymers.

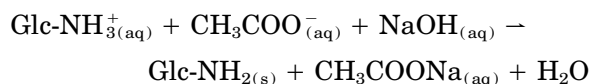
ple of a well-studied system is that of viscose fibers, where a chemical reaction is involved in the coagulation step. In this case, cellulose is regenerated by the transformation of alkaline sodium cellulosexanthogenate into free xanthogenic acid and then into cellulose hydrate—all in the presence of bivalent metal ions such as  $Zn^{2+}$  or  $Cd^{2+}$ . Another example of a coagulation bath involving a chemical reaction with the polymer is formaldehyde dissolved in a polyvinyl alcohol dope solution. When the dope solution comes into contact with a base, the formaldehyde reacts with hydroxyl groups in the polymer chains to form bridges or crosslinks between the chains.<sup>2</sup>

As early as 1947, it was shown by Hermans,<sup>3</sup> and later by Paul in 1968<sup>4</sup> and Liu et al. in 1989,<sup>5</sup> that a sharp boundary line is associated with the phenomenon of diffusion of various substances into polymer solutions. The coagulation of chitosan in acetic acid involves a similar process based on a simple acid-base reaction. If, for example, chitosan ( $Glc-NH_2$ ) is dissolved in a weak solution ( $\sim 1-5\%$ ) of acetic acid and then brought into contact with a strong basic solution such as 1M aqueous sodium hydroxide, the proton exchange between acid and base will bring about the precipitation of the polymer. The mechanism of a such a reaction is as follows<sup>8</sup>:

Step 1



Step 2



When a cross-section of a solution-spun fiber is taken in the initial stages of the coagulation process, two concentric circles are observed: the outer or “skin” being hard, solid and almost 100% polymer and the inner circle or “core” being the viscous solution of the polymer dissolved in the acidic solvent. A distinct boundary between the precipitated and the dissolved polymer is apparent and forms the division between the solidified and unsolidified polymer (the “two concentric circles”). This is shown schematically in Figure 2. Such a boundary must be intimately related to the reaction between solvent and nonsolvent in the coagulation bath. With time, the boundary moves inward until it reaches the center of the fiber and all of the polymer is precipitated. With increasing temperature, the rate at which this boundary moves inward increases. Ziabicki, in 1976, detailed the theory related to such a boundary motion and also detailed some related experimental results.<sup>2</sup>

The objective in this study was to determine how long a 5% chitosan solution, in fiber form, should spend in the coagulation bath in order to arrive at a completely coagulated filament. In their 1994 review paper on chitin and chitosan as fiber and film formers, Rathke and Hudson have stated that there is a lack of comparative coagulation studies regarding chitosan.<sup>6</sup> More specifically, Cuculo and coworkers have presented a series of articles detailing coagulation studies for cellulose in the ammonia/ammonium thiocyanate solvent system. These studies involved making large-scale (cigar-sized) gelled rods of the cellu-

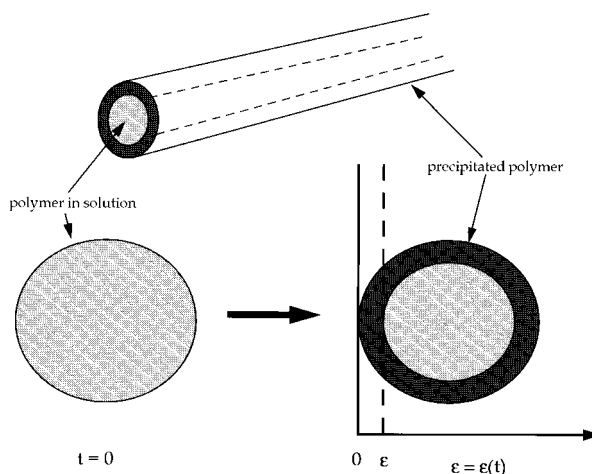


**Figure 2** A schematic illustration of boundary motion with time in the cross-section of a cylindrical-shaped polymer during the coagulation step.

lose dope solution. These rods were individually immersed in differing coagulants. Time, temperature, and concentration were also varied sequentially. The rods were removed from the coagulant after the given period and cross-sectioned into discs so that the boundary motion could be analyzed under a microscope. This study on the chitosan/acetic acid system follows a technique similar to that of Cuculo and coworkers; however, we have taken samples of actual fibers and examined them using a much higher power digitizing microscope and image-analyzing software (models and brand names are detailed under the "Method" section). Not only have we more closely modeled a commercially useful fiber, we have been able to obtain reproducible diffusion of 70% of the radius of the fiber compared with only 30% using the gelled rods method of Liu and coworkers.<sup>5</sup>

## EXPERIMENTAL

### Materials

Chitosan, lot #740026, was obtained as a 60 mesh powder from Pronova Biopolymer (Raymond, WA). This batch was a crab-based chitosan with a claimed viscosity of 1,000 mPas. The following chemicals were all obtained and used as reagent grade from either Sigma Chemical Co. or Aldrich: glacial acetic acid, sodium hydroxide pellets, ethanol, potassium hydroxide flakes, ammonium hydroxide, lithium hydroxide powder, trisodium orthophosphate powder, and sodium bicarbonate powder.

### Chitosan Characterization

#### Degree of Deacetylation

The degree of deacetylation (DA) of the chitosan was verified using a method of ultraviolet spectrophotometry as developed by Muzzarelli et al.<sup>7</sup> The main absorbance occurred in the range of 200–204 nm, and the DA value was found to be  $84.9 \pm 0.2\%$ .

#### Molecular Weight

The average molecular weight,  $M_v$ , was determined based on intrinsic viscosity, as measured in a Ubbelohde viscometer with a solvent of 0.1M acetic acid/0.2M NaCl, and was calculated to be  $7.73 \times 10^5$  g mol<sup>-1</sup>. This was calculated based on the Mark-Houwink equation

$$[\eta] = KM^\alpha \quad (1)$$

where  $\alpha = 0.93$  and  $K = 1.81 \times 10^{-5}$  g/dL, as outlined by Rinaudo and Domard.<sup>8</sup> The method for this measurement followed the procedure outlined in Pronova Quality Assurance Code 750 for the determination of the average viscosity molecular weight of chitosan. The experiment was repeated three times with five dilutions for each run.

The value for the average molecular weight was supported using high-pressure liquid chromatography (HPLC), as outlined by Wu.<sup>9</sup> Components of the HPLC system included a mobile phase of 2% acetic acid; a sodium polystyrene sulfonate standards calibration kit from Scientific Polymer Products Inc., with an  $M_w$  range of 4,000–1,200,000; a biosep-sec-s4000, stainless steel column (Phenomenex) measuring  $300 \times 7.8$  mm; a Shimadzu LC-6A pump; and a Shodex refractive index detector. The molecular weight distribution of chitosan sample 740026 using the HPLC technique was  $M_n 5.32 \times 10^4$  g mol<sup>-1</sup>,  $M_w 1.14 \times 10^5$  g mol<sup>-1</sup>, and average dispersity 2.33.

### Chitosan Solution Preparation

A 5% chitosan solution was chosen because a 4% or lower concentration solution is too low in viscosity for practical spin applications, and at concentrations of 7% and higher, the viscosity is too high for solution extrusion. For the wet spinning of chitosan fibers, a 5% concentration was observed to give better wet strength over a 6% solution, and thus, a concentration of 5% was chosen. The best solvent concentration of acetic acid was found to be 2%, because anything lower was not sufficient for dissolution and anything higher tended to demonstrate an undesirable salting-out effect of the chitosan. All solutions were prefiltered to 3  $\mu$ m. The viscosity of each solution was recorded using a Brookfield RVDV II+ digital viscometer. These values were typically around 10,000 centipoise (see Table I).

### Method of Coagulation and Boundary Measurement

Chitosan solutions were placed into 30-mL plastic syringes that had an inside spout diameter of 1.9 mm. Needles were not attached to the syringes. The syringes were then placed into a #365 Sage syringe pump, and the solutions were extruded into an acrylic tray containing the coagulant. Im-

**Table I Characteristics of Different Chitosan Solutions Used in Experiments Involving Boundary Motion Versus Time**

Sample	Origin	Degree of DA (%)	Solution Configuration	Solution Viscosity (cP)
Chitosan A	Pronova lot #740026	85.0	5% chitosan/ 2% acetic acid	10 360 $\pm$ 200
Chitosan B	Grand Banks	83.8	1.5% chitosan/ 2% acetic acid	12 200 $\pm$ 40
Chitosan C	North Pacific Ocean	80.7	3% chitosan/ 2% acetic acid	14 380 $\pm$ 40

mediately after contact with the coagulant, the polymer began to precipitate. The hardened shape was pinched off with tweezers such that each sample was  $\sim 2.5$  cm in length; in the coagulation bath, the sample was held steady and not allowed to move through the bath. The temperature of the coagulation bath was adjusted and maintained using a submerged stainless steel heating coil with an accuracy of  $\pm 0.1^\circ\text{C}$ . The temperature was monitored using a thermocouple probe at the site where the sample was held submerged in the bath. After the allotted time, the sample was removed from the bath and immersed in a buffer bath, at a pH of  $\sim 11$ , containing a 1M sodium bicarbonate solution. Immediately thereafter, the sample was frozen in liquid nitrogen. After arrival at the imaging facility, samples were removed and cross-sectioned by hand using a razor blade. These cross-sections were viewed under a Leitz Diaplan microscope with a 2.5 objective lens. An HV-CIO CCD Hitachi camera was used to digitize each cross-section image. The software used to analyze the digitized images was an MCID M2 made by Imaging Research Inc. Calibration of the measuring program was achieved using a reticle grid.

A distinct boundary between coagulated and uncoagulated polymer was readily apparent. The depth,  $\varepsilon(t)$ , to which the coagulated skin had reached toward the center was determined by comparing the inner radius of the fluid, or dissolved polymer, to the outer diameter of the precipitated polymer. The outer diameter of each extruded sample was larger than the hole diameter of the syringe but did not vary significantly between the various samples. In other words, the extruded samples tended to swell on interaction with the coagulant; this point is discussed in more detail in the next section. All of the extruded samples possessed outside diameters of  $2.45 \pm 0.20$  mm.

Three separate sets of experiments were conducted. In the first group of experiments, time was varied for several different coagulants, from 22 sec to 2 min, while the temperature in the coagulation bath was held constant at  $23 \pm 0.3^\circ\text{C}$ . In the second round of experiments, temperature was varied from 20 to  $70^\circ\text{C}$ , also for different coagulants, while the time was kept constant at  $45 \pm 1$  sec. In the final set of experiments, three different chitosans were analyzed. A 1M NaOH coagulant was used, and time was varied from 22 sec to 2 min at  $23 \pm 0.3^\circ\text{C}$ . The characteristics of the three chitosans are listed in Table I. Chitosan type A was the only type of chitosan used in the first and second sets of experiments.

## RESULTS AND DISCUSSION

### Boundary Motion as It Relates to Time

The boundary movement as it relates to time has been observed for several different coagulants. Figure 3(a) graphically illustrates these results and demonstrates a straight line relationship between boundary position,  $\varepsilon(t)$ , and the square root of time spent in the coagulation bath. The explanation behind this relationship is in accordance with Fick's 2nd Law. Ziabicki<sup>2</sup> has modeled the theory of diffusion with a moving boundary in wet-spinning by assuming a linear, one-dimensional system containing component  $b$  into which the other component  $a$  migrates from the outside and instantaneously reacts with  $b$ . The respective diffusion coefficients are  $D_a$  (component  $a$  in the reacted—or solid, polymer skin—layer) and  $D_b$  (component  $b$  in the unreacted—or polymer in solution core—layer). Accordingly, the rate of mass transfer between the reacted and unreacted layers can be illustrated using two Fickian differential equations:

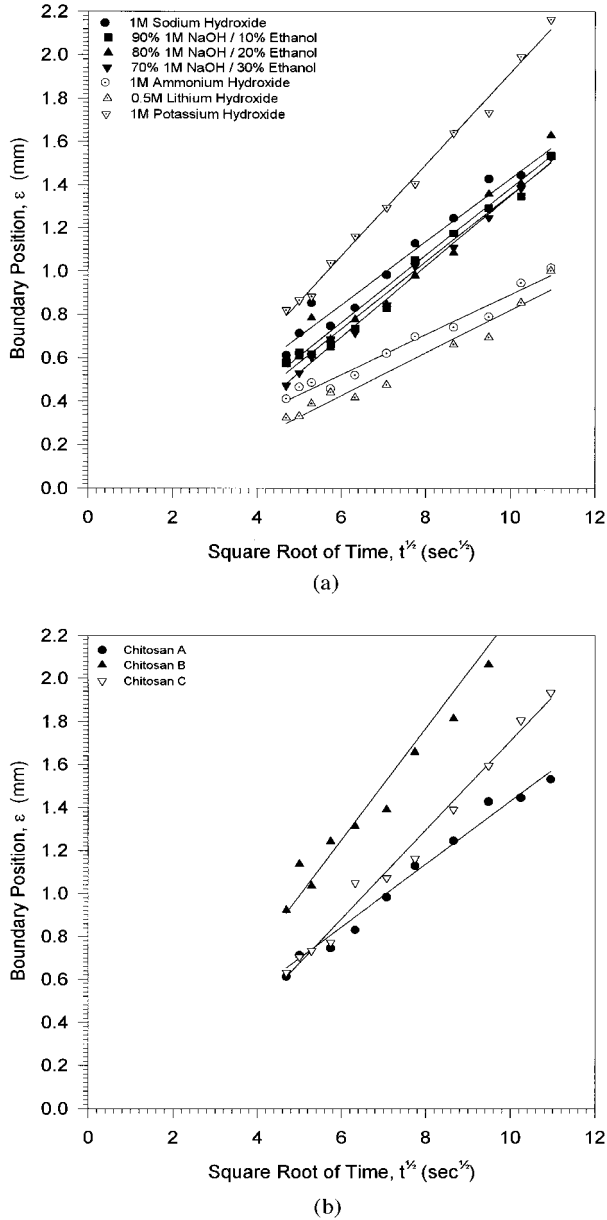


**Figure 3** (a) Adherence to Fick's Law when boundary motion is compared with the square root of time for chitosan A in varying coagulants. (b) Adherence to Fick's Law when boundary motion is compared with the square root of time for different chitosans in 1M NaOH.

$$\text{Reacted layer: } \quad \partial C_a / \partial t = D_a (\partial^2 C_a / \partial x^2) \quad (2a)$$

$$(0 < x < \varepsilon)$$

$$\text{Unreacted layer: } \quad \partial C_b / \partial t = D_b (\partial^2 C_b / \partial x^2) \quad (2b)$$

$$(\varepsilon < x < \infty)$$

where  $x$  is the distance measured from the outside

surface of the reacted layer,  $\varepsilon$  is the position of the boundary line, and  $C$  is the concentration of the diffusing species.

In order to arrive at a solution to eqs. (2a) and (2b), the following assumptions are made:

- i. That the solidification of chitosan in acetic acid involves a chemical reaction and the resulting production of water. This mechanism has been outlined above in the introduction section. The production of water was further evidenced by the swelling of the polymer samples during the coagulation step, and the subsequent reduction in volume if the samples were allowed to air dry.
- ii. That there is no diffusion of the acid or solvent from the liquid core to the solidified polymer. The coagulant migrates (i.e., from outside the sample) through the solidified layer to the boundary where solid polymer meets liquid polymer. There, it reacts with the acid to form solid polymer. So then, while the  $\text{OH}^-$  ions diffuse through the solid polymer to the boundary, the  $\text{H}^+$  ions likely do not diffuse out of the liquid center at all. Instead, they only make it as far as the boundary, where they instantaneously react with the base. This supposition is based on the fact that the concentration of the coagulant is much greater than that of the solvent.

Based on these assumptions, the acid, component  $b$ , is not diffusing out of the polymer at all. If this is the case, then  $D_b$  in eq. (2b) goes to zero and the boundary conditions for solving eq. (2a) are as follows:

$$C(0, t) = C_{a,0} \quad C(\varepsilon, t) = C_{a,0} \quad C(x, 0) = 0$$

Based on these boundary conditions, the solution to eq. (2a) is

$$C_a - C_{a,0} / C_{a,0} = \text{erf}[\varepsilon / (2\sqrt{tD})] \quad (3)$$

where  $C_{a,0}$  is the initial and known concentration of component  $a$ ,  $C_a$  is the concentration of  $a$  at some distance  $x$  from the surface of the sample, and  $\varepsilon$  has been substituted for  $x$  to consider diffusion at the boundary.<sup>10</sup>

Equation 3 illustrates that for the case of diffusion into a semi-infinite medium exhibiting zero initial concentration and a constant concentration

at the surface, the single dimensionless parameter

$$\varepsilon/(2\sqrt{tD}) \quad (4)$$

is a constant value. It follows from this derivation that the amount of penetration of the diffusing substance is proportional to the square root of time. This property holds in a semi-infinite medium so long as the initial concentration is uniform and the surface concentration remains constant.<sup>11</sup>

In Paul's 1968 results involving a copolymer of acrylonitrile and vinyl acetate, it was evident that this linear relationship between boundary position and time was valid until 30% penetration, after which Paul's results begin to deviate from linearity.<sup>4</sup> The results of Figure 3(a) do show, in all cases, that Fick's Law for a semi-infinite medium is valid until at least 72% penetration by the coagulant of the sample. It is probable that at some point, the semi-infinite model will become invalid. When the basic ions migrate to positions very close to the center of the sample, Fick's 2nd Law based on a model such as a cylindrical model would likely describe the process more closely. Because the size of the migrating species is several orders of magnitude smaller than the size of the sample, this is not expected to happen until the migrating species is very close to the center of the sample. Deviations from linearity after 72% penetration, as seen in Figure 3(a), are more likely to be as a result of a pH change within the sample. The production of the water, as a result of the acid/base reaction, could be enough to cause a pH change in the coagulant.

Paul has labeled the term  $(\varepsilon/\sqrt{t})$  as the "coagulation rate."<sup>4</sup> Table II presents the "coagulation rate" values for each agent, along with regression values, standard deviations, and corresponding molecular volumes. Figure 4 contains digital images displaying boundary motion with time.

One approach to the analysis of the data presented in Figure 3(a) is to consider the role of the molecular size and structure of the coagulant. In other words, what might be some of the barriers or the proponents to the solvent/nonsolvent exchange process? According to Liu et al.,<sup>5</sup> a linear relationship does exist between the diffusion coefficient of a spherical particle and its molecular volume. The development is as follows.

The Stokes-Einstein equation relates the diffusion coefficient of a spherical particle to its radius as

$$D = RT/(6\pi\eta Nr_0) \quad (5)$$

where  $\eta$  is the viscosity of the medium,  $N$  is Avogadro's number,  $T$  is the temperature, and  $r_0$  is the radius of the diffusing particles. Inserting the relation,  $V = (\frac{4}{3})\pi r_0^3 N$ , into eq. (5) and taking natural logarithms yields

$$\ln D = \ln RT/6\pi\eta N + 18.7 - \frac{1}{3} \ln V \quad (6)$$

For a diffusion process involving constant viscosity and constant temperature, eq. (6) can be more simply written as

$$\ln D = c - \frac{1}{3} \ln V \quad (7)$$

where  $c$  is a constant.

Barrow contests that molecules do not necessarily obey Stokes' Law, even if they are spherical.<sup>12</sup> To examine Stoke's Law in our system, eq. (7) has been substituted with Fick's Law as follows:

$$\varepsilon/(2\sqrt{tD}) = c' \quad (4)$$

where  $c'$  is a constant.

$$\varepsilon/(\sqrt{tD}) = c' \quad (4a)$$

$$D = [\varepsilon/(\sqrt{tc'})]^2 \quad (4b)$$

Substituting eq. (4b) into eq. (7)

$$\ln \varepsilon^2/[t(c')^2] = c - \frac{1}{3} \ln V \quad (7b)$$

and simplifying the equation by combining the constants into one constant,  $c$ ,

$$\ln \varepsilon^2/t = c - c/3 \ln V \quad (7c)$$

Figure 5 illustrates a plot of  $\ln \varepsilon^2/t$  versus  $\ln V$  for chitosan A samples in several different coagulants after 60 sec at room temperature. The values were generated from Table II. A straight line relationship is seen for the smaller coagulants, which suggests that Stoke's Law is valid for small, spherical coagulants. The regression analysis value of the line is 0.8905. The trisodium orthophosphate coagulant, while plotted, was not included in the regression analysis. An explanation for its large divergence from the other coagulants could be its relatively large molecular volume and

**Table II Experimental Values of  $(\epsilon/\sqrt{t})$  of Solutions of 5% Chitosan/2% Acetic Acid in Various Coagulants at  $23 \pm 0.3^\circ\text{C}$** 

Coagulant (Type of Chitosan; See Table I)	$(\epsilon/\sqrt{t}) \times 10^{-3}$ ( $\text{cm s}^{-1/2}$ )	Regression Values ( $r$ ) <sup>a</sup>	Standard Deviations <sup>b</sup>	Molecular Volume, $V \times 10^3$ ( $\text{mm}^3 \text{mol}^{-1}$ ) <sup>c</sup>
1M NaOH (A)	0.141	0.968	0.012	38.37
90% NaOH/10% ethanol (A)	0.155	0.992	0.007	40.37
80% NaOH/20% ethanol (A)	0.156	0.979	0.011	42.37
70% NaOH/30% ethanol (A)	0.164	0.997	0.004	44.37
1M $\text{NH}_4\text{OH}$ (A)	0.092	0.987	0.005	35.42
0.5M $\text{Na}_3\text{PO}_4 \cdot 12\text{H}_2\text{O}$ (A)	0.053	0.901	0.009	234.64
1M KOH (A)	0.211	0.997	0.005	53.62
0.5M LiOH (A)	0.099	0.977	0.006	16.40
1M NaOH (A)	0.141	0.968	0.012	38.37
1M NaOH (B)	0.141	0.968	0.011	38.37
1M NaOH (C)	0.207	0.994	0.009	38.37

<sup>a</sup> Values obtained using a linear regression program in Sigma Plot<sup>®</sup>.

<sup>b</sup> Values also obtained using a regression analysis in Quattro Pro<sup>®</sup>.

<sup>c</sup> Defined as the volume occupied by 1 mol. Numerically equal to the molecular weight divided by the density determined at  $20^\circ\text{C}$ .<sup>20</sup>

complex nature. This excessive volume would obviously be a natural barrier to diffusion in the polymer network.

#### Boundary Motion as It Relates to Time for Different Chitosans

Experiments involving changes in temperature were not attempted in this section of the study. The time experiments followed exactly the same method as that outlined above under "Boundary Motion as It Relates to Time." Three chitosans were considered: two from separate suppliers on the northern Pacific Coast of the United States and one from the Grand Banks just off the east coast of Canada. Figure 3(b) illustrates the results, and the numerical results are listed at the bottom of Table II. All of the chitosans were dissolved in solution so as to give individual solutions with final viscosities that were in the neighborhood of 10,000 cP. Table I lists the characteristics of three different chitosan solutions.

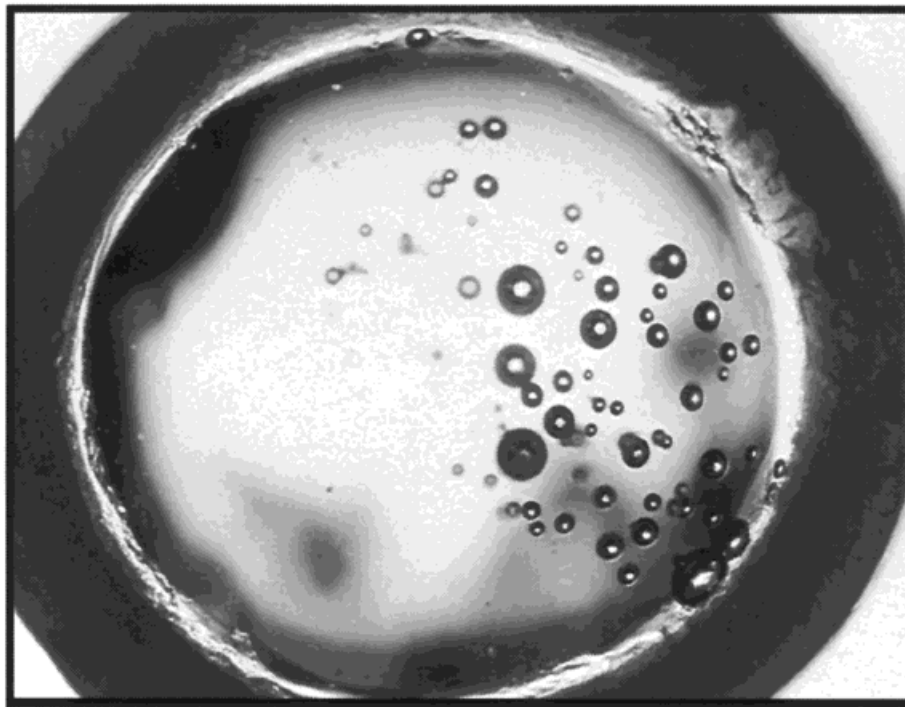
The results shown in Figure 3(b) demonstrate that chitosans of differing origins will precipitate at different rates. Indeed, chitosan A, originating from the Grand Banks, gives the most rapid rate of coagulation of the three chitosans tested. However, all of the chitosans were shrimp based and their respective properties of degree of DA and solution viscosity in acetic acid were virtually the same (see Table I). It is likely that the rate of

coagulation is more affected by the method of DA than by the origin of the chitosan itself.

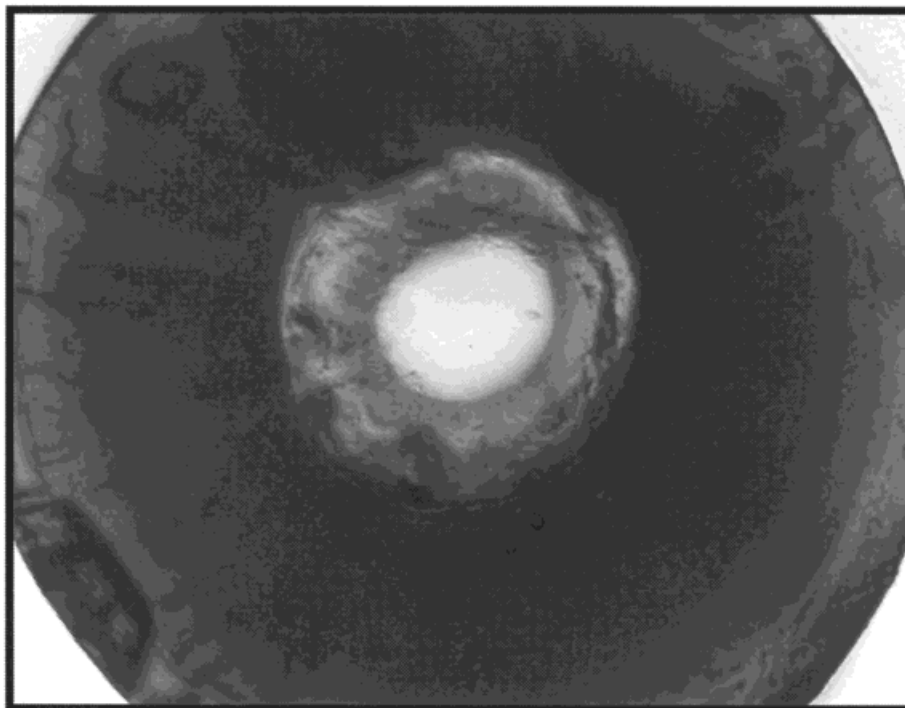
There are some references to this suggestion. In particular, the work of Värum and coworkers in 1991<sup>13</sup> supported the earlier findings of Kurita and coworkers in 1977.<sup>14</sup> Chitosan is not a homopolymer. Rather, it is a copolymer made up of units of 2-acetamido-2-deoxy- $\beta$ -D-glucopyranose (GlcNAc) and 2-amino-2-deoxy- $\beta$ -D-glucopyranose (GlcN). The proportions of the two monomers are based on the extent of the DA. The distribution of the different monomer units is based on the method of DA. Both research groups displayed evidence that chitosans processed by *N*-deacetylation under heterogeneous conditions (50%  $\text{NaOH}_{(\text{aq})}$  at  $70^\circ\text{C}$ ) produced a slightly more blockwise distribution than those prepared under homogeneous conditions (10%  $\text{NaOH}_{(\text{aq})}$  at  $25^\circ\text{C}$ ). In addition, chitosans having a more random nature than block form were also found to be more amorphous and to have better solubility.

#### Boundary Motion as It Relates to Temperature (Calculation of Activation Energy)

It is generally accepted that the coagulation of a dissolved polymer in a solvent/nonsolvent exchange bath is a rate process. In many systems, the mobility of molecules and ions increases with increasing temperature. As such, this rate process is also temperature dependent.<sup>15</sup> In polymer sys-



(a)



(b)

**Figure 4** (a) Cross-section of cylindrical chitosan sample after 28 sec of submersion in 70% 1M NaOH/30% ethanol. (b) Cross-section of cylindrical chitosan sample after 120 sec of submersion in 70% 1M NaOH/30% ethanol.



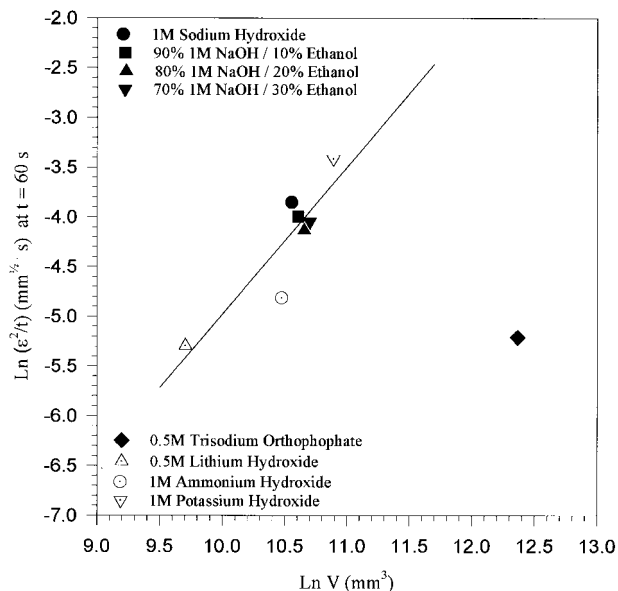


**Figure 5** The dependence of diffusion rate at 60 sec on the molecular volume of different coagulants at room temperature. The data can be found in Table I.

tems, we are specifically concerned with the migration of atoms/ions or small molecules between the long polymer chains. (Selective diffusion through polymer membranes is used in several new drug delivery systems.<sup>16</sup>) The diffusing atoms, ions, or molecules penetrate between the polymer chains as opposed to transiting from one position to another within the chain structure. The diffusion rate will increase through the chain structure when the migrating species is smaller or when larger voids are present between the chains.

The ability of atoms, ions, or molecules to diffuse increases as the temperature, or thermal energy, possessed by the mobile species increases. The rate of motion is related to temperature or thermal energy by the Arrhenius equation:

$$\ln(\text{rate}) = \ln(c_0) - Q/RT \quad (8)$$

where  $c_0$  is a constant,  $T$  is the temperature, and  $Q$  is the activation energy required to allow the particle to transit. The equation is based on a statistical analysis of the probability that the migrating species will have the supplemental energy  $Q$  necessary to cause motion. The rate is related to the number of particles that move. If a plot of  $\ln(\text{rate})$  of some reaction versus  $1/T$  is made, the slope of the curve will be  $-Q/R$ , and as a result,  $Q$  can be calculated. The constant  $c_0$  is simply the intercept when  $1/T$  is zero.<sup>17</sup>

The boundary movement for the precipitation of chitosan in 1M KOH, 1M NH<sub>4</sub>OH, 70% 1M NaOH/30% ethanol, 0.5M LiOH, and 0.5M trisodium orthophosphate was observed for temperatures varying from 20 to 70°C. The submersion time was  $45 \pm 1$  sec at each temperature. Figure 6 presents an Arrhenius plot of  $\ln(\text{coagulation rate})$  versus the inverse temperature. As expected, the coagulation rate increased with increasing temperature and a linear relationship is exhibited in accordance with the Arrhenius theory. Table III presents the associated regression equations, correlation coefficients, and activation energies for the different coagulants tested. The calculated activation energies are within the same order of magnitude as those reported for other coagulation systems such as cellulose/NH<sub>3</sub>/NH<sub>4</sub>SCN in methanol, 1-propanol, and 2-propanol ( $5.146\text{--}16.024$  kJ mol<sup>-1</sup>); polyacrylonitrile/DMF solution in an aqueous DMF bath ( $15.899\text{--}25.941$  kJ mol<sup>-1</sup>); and cellulose xanthate/NaOH in an aqueous H<sub>2</sub>SO<sub>4</sub> bath ( $7.866$  kJ mol<sup>-1</sup>).<sup>5</sup>

If one considers that the mobility of the diffusing species (the coagulant) is affected by the size of its molecule and by the size of the holes in the molecule into which it is diffusing (the polymer), then KOH should exhibit a relatively higher activation energy in comparison to the other coagulants. This is, however, not the case. Liu et al.<sup>5</sup>

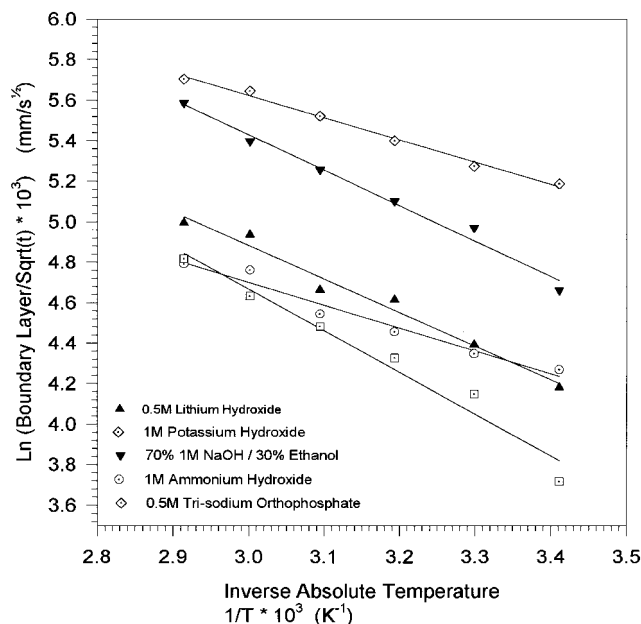


**Figure 6** An Arrhenius plot for boundary motion versus temperature for chitosan A in various coagulants. The temperature was varied from 20 to 70°C.

**Table III** Calculated Activation Energies, Regression Equations, and Correlation Coefficients for 5% Chitosan/2% Acetic Acid Precipitating in Various Coagulants at Varying Temperatures

Coagulant	Regression Equation <sup>a</sup>	<i>r</i>	<i>Q</i> (kJ mol <sup>-1</sup> ) <sup>b</sup>	Standard Deviation for <i>Q</i> <sup>c</sup>
70% 1M NaOH/ethanol	$\ln(\varepsilon/t \cdot 10^3) = 9.477 - (1.345 \cdot 10^3/T)$	0.990	11.184	0.112
1M KOH	$\ln(\varepsilon/t \cdot 10^3) = 8.920 - (1.098 \cdot 10^3/T)$	0.996	9.134	0.048
1M NH <sub>4</sub> OH	$\ln(\varepsilon/t \cdot 10^3) = 8.095 - (1.131 \cdot 10^3/T)$	0.982	9.406	0.110
0.5M Trisodium orthophosphate	$\ln(\varepsilon/t \cdot 10^3) = 10.851 - (2.061 \cdot 10^3/T)$	0.983	17.133	0.191
0.5M LiOH	$\ln(\varepsilon/t \cdot 10^3) = 9.860 - (1.659 \cdot 10^3/T)$	0.999	13.790	0.962
Literature Values				
Cellulose/NH <sub>3</sub> /NH <sub>4</sub> SCN in methanol, 1-propanol, and 2-propanol			5.148–16.024	
Polyacrylonitrile/DMF in DMF(aq)			15.899–25.941	
Cellulose xanthate/NaOH in H <sub>2</sub> SO <sub>4</sub>			7.866	

<sup>a</sup> Regression equations and *r* values in column to the right obtained using SigmaPlot<sup>®</sup>.

<sup>b</sup> These literature values can be found in reference 5.

<sup>c</sup> Values calculated using regression analysis available in QuatroPro<sup>®</sup>.

concluded that intermolecular forces between coagulant and solvent may play a more prominent role in determining this energy barrier to diffusion than does molecular volume. It may be that a strong affinity between the acid solvent and the basic potassium hydroxide leads to its lower activation energy.

It is not surprising that trisodium orthophosphate, with its relatively large molecular weight and correspondingly large molecular volume (see Table II), would exhibit such a large activation energy (see Table III). One can only speculate as to the nature of the mechanism governing the diffusion exchange taking place between chitosan and the coagulant. If the process is managed by a vacancy mechanism, the most common of all diffusion mechanisms,<sup>18</sup> then there is no doubt that the size of the migrating species plays a key role in both the value of the activation energy and the level of the coagulation rate. According to Liu et al., the effect of the molecular size of the coagulant is mainly on the diffusion coefficient of the coagulant.<sup>19</sup>

#### Errors in the Method

For each given time and temperature, three samples were extruded. A random error was associated with the time spent in the coagulant because the precision of the handheld timer was only good

to  $\pm 1.0$  sec. A random error must also be associated with the temperature of the bath because the precision of the temperature control was good only to  $\pm 0.1^\circ\text{C}$ . For each one of the three samples, three separate cross-sections were made and analyzed under the microscope. Cross-sections viewed under the microscope were digitized for later measurement using the computer software. The precision with which the software could measure diameters was within  $\pm 0.01 \mu\text{m}$ . The combination of the software precision and the precision of the timing instrument reduced the accuracy of the results in Tables II and III to three decimal places.

#### CONCLUSIONS

The depth of boundary movement  $\varepsilon(t)$  was found to be directly proportional to the square root of time, for each coagulant tested. This was in accordance with Fick's 2nd Law. A linear relationship between the molecular volume of the coagulant and the diffusion rate of the coagulant has been demonstrated.

In a second set of experiments, the activation energies for five of the coagulants were also calculated with the following results: 70% 1M NaOH/30% ethanol at 11.184 kJ mol<sup>-1</sup>, 1M KOH at 9.134 kJ mol<sup>-1</sup>, 1M NH<sub>4</sub>OH at 9.406 kJ mol<sup>-1</sup>, 0.5M LiOH at 13.790 kJ mol<sup>-1</sup>, and 0.5M triso-

dium orthophosphate at  $17.133 \text{ kJ mol}^{-1}$ . Of all of the coagulants tested,  $1 \text{ M}$  KOH yielded complete coagulation after 2 min at  $23^\circ\text{C}$  and after 45 sec at  $60^\circ\text{C}$ .

In the third and last group of experiments, three different chitosans originating from three different locations were analyzed in  $1 \text{ M}$  NaOH. Chitosan A from the Grand Banks gave the most rapid rate of coagulation. Further, it is theorized that the rate of coagulation was more affected by the method of DA than by the origin of the chitosan itself.

## REFERENCES

1. F. Shahidi, *Canadian Chemical News*, **Sept.**, 25 (1995).
2. A. Ziabicki, *Fundamentals of Fibre Formation*, Wiley, London, 1976.
3. J. J. Hermans, *J. Colloid Sci.*, **1**, 387 (1947).
4. D. R. Paul, *J. Appl. Polym. Sci.*, **12**, 383 (1968).
5. C.-K. Liu, J. A. Cuculo, and B. Smith, *J. Polym. Sci. Polym. Phys. Ed.*, **27**, 2493 (1989).
6. T. D. Rathke and S. M. Hudson, *J.M.S.—Rev. Macromol. Chem. Phys.*, **C34**, 375 (1994).
7. R. A. A. Muzzarelli, C. Jeuniaux, and G. W. Gooday, *Chitin in Nature and Technology*, Plenum, New York, 1986.
8. M. Rinuado and A. Domard, *Proceedings of the Fourth Conference on Chitin and Chitosan*, Trondheim, Norway, 1988.
9. A. C. M. Wu, *Methods Enzymol.*, **161**, 447 (1988).
10. C.-K. Liu, Doctoral Thesis, N.C. State University, Raleigh, 1985.
11. J. Crank, *The Mathematics of Diffusion*, 2nd Ed., Oxford University Press, Oxford, 1976.
12. G. M. Barrow, *Physical Chemistry*, 5th Ed., McGraw-Hill Book Co., New York, 1988.
13. K. M. Vårum, M. W. Anthonsen, H. Grasdalen, and O. Smidsrod, *Carbohydrate Res.*, **211**, 17 (1991).
14. K. Kurita, T. Sannan, and Y. Iwakura, *Makromol. Chem.*, **178**, 3197 (1977).
15. S. B. Tuwiner, *Diffusion and Membrane Technology*, Reinhold Publishing Corp., London, 1962.
16. J. H. Kim, et al., *J. Appl. Polym. Sci.*, **44**, 1823 (1992).
17. D. R. Askeland, *The Science and Engineering of Materials*, 3rd Ed., PWS Publishing Co., Boston, 1994.
18. R. J. Borg and G. J. Dienes, *An Introduction to Solid State Diffusion*, Academic Press Inc., San Diego, 1988.
19. C.-K. Liu, J. A. Cuculo, and B. Smith, *J. Polym. Sci. Part B Polym. Phys.*, **28**, 449 (1990).
20. R. C. Weast, *CRC Handbook of Chemistry and Physics*, 68th Ed., CRC Press Inc., Boca Raton, FL, 1987–88.